

Electrorheological properties of suspensions of hollow globular titanium oxide/polypyrrole particles

M. Sedlačik · M. Mrlík · V. Pavlínek · P. Sába ·
O. Quadrat

Received: 29 April 2011 / Revised: 21 September 2011 / Accepted: 22 September 2011 / Published online: 6 October 2011
© Springer-Verlag 2011

Abstract Hollow globular clusters of titanium oxide (TiO₂) nanoparticles were synthesized by a simple hydrothermal method. The prepared particles were consequently coated by in situ polymerization of conductive polymer polypyrrole (PPy) to obtain novel core–shell structured particles as a dispersed phase in electrorheological (ER) suspensions. The X-ray diffraction analysis and scanning electron microscopy provided information on particle composition and morphology. It appeared that PPy coating improved the compatibility of dispersed particles with silicone oil which results in higher sedimentation stability compared to that of mere TiO₂ particles-based ER suspension. The ER properties were investigated under both steady and oscillatory shears. It was found that TiO₂/PPy particles-based suspension showed higher ER activity than that of mere TiO₂ hollow globular clusters. These observations were elucidated well in view of their dielectric spectra analysis; a larger dielectric loss enhancement and faster interfacial polarization were responsible for a higher ER

activity of core–shell structured TiO₂/PPy-based suspensions. Investigation of changes in ER properties of prepared suspensions as a function of particles concentration, viscosity of silicone oil used as a suspension medium, and electric field strength applied was also performed.

Keywords Electrorheology · Titanium oxide · Hollow globular clusters · Polypyrrole coating · Core–shell particles · Dielectric properties

Introduction

Electrorheological (ER) behavior of suspensions of electrically polarizable particles dispersed in an insulating fluid has been the object of investigations of many researchers in the past. The ability to suddenly change rheological properties due to formation of a stiff chain-like structure of polarized particles in the electric field ranges these fluids among smart materials with a great potential in engineering applications [1–3]. The nature of this effect enabling the remote-controlled transition from liquid to quasi-solid state has been discussed in review articles [4–7]. The broader using of ER effect in practice is still hindered by several problems such as low polarization forces and temperature dependence, leaking current through the suspension and particle sedimentation. To overcome these drawbacks, various ER materials differing in shape [8] and organic [9, 10] or inorganic [11] nature have been developed. In addition, a dispersed phase of particles with modified structure as metal-doped titania [12], polymer/inorganic hybrid [13, 14], and core–shell composites [15] have also been used in ER fluids.

It is well known that the interfacial polarization takes dominant role in determination of the ER performance, and

M. Sedlačik · M. Mrlík · V. Pavlínek · P. Sába
Centre of Polymer Systems, University Institute,
Tomas Bata University in Zlin,
Nad Ovcirnou 3685,
760 01 Zlin, Czech Republic

M. Sedlačik (✉) · M. Mrlík · V. Pavlínek · P. Sába
Polymer Centre, Faculty of Technology,
Tomas Bata University in Zlin,
náměstí T. G. Masaryka 275,
762 72 Zlin, Czech Republic
e-mail: msedlacik@ft.utb.cz

O. Quadrat
Institute of Macromolecular Chemistry,
Academy of Sciences of the Czech Republic,
Heyrovsky Sq. 2,
162 06 Prague 6, Czech Republic

dielectric and electric properties of particles are main factors affecting the ER activity. At present great attention has been paid to titanium oxide (TiO_2) because of its high dielectric constant. Its weak ER activity mainly originating from its low active natural structure could be improved by changing its molecular or crystalline structure or microstructure [16]. In this study, with a view to prepare a novel material with good ER performance, the hollow globular clusters of titanium oxide nanoparticles coated with a polypyrrole (TiO_2/PPy) were synthesized and steady-state and oscillatory flow behavior of their silicone oil suspensions related to dielectric properties were analyzed.

Experimental

Materials

Potassium titanium oxide oxalate dihydrate (TiO) (OCO-COOK)₂; PTO, technical grade), hydrogen peroxide solution (H_2O_2 , 30 wt.%), hydrochloric acid (HCl , $\geq 37\%$), pyrrole (Py , $\geq 98\%$) and ammonium persulfate (APS, 98%) were purchased from Sigma–Aldrich Incorporation (St. Louis, USA). Cetyltrimethylammonium bromide (CTAB, 98%) was obtained from Lach–Ner, s.r.o. (Neratovice, Czech Republic). All chemicals were used without further purification.

Synthesis of TiO_2/PPy particles

The mere TiO_2 hollow clusters were prepared according to the report [17], with a minor modification. PTO 1.416 g (4 mmol) was dissolved in 30 ml of distilled water and to a dark red solution 30 ml of 30% H_2O_2 and 3 ml of 37% HCl were added. The mixture was transferred to a 100-ml Teflon-lined autoclave and filled up with distilled water up to 90% of the total volume. The autoclave was sealed, heated at 150 °C for 8 h, and cooled down to room temperature. The suspension of TiO_2 clusters was filtered, the precipitate rinsed with distilled water several times, and dried at 60 °C in the vacuum for 6 h. The yield was around 83% (approximately 0.281 g).

To obtain TiO_2/PPy particles, 1.845 g of CTAB was dissolved in 100 ml of distilled water and 2 g of TiO_2 clusters was added. The suspension was sonicated for 30 min and cooled to 0–5 °C during vigorous stirring. Then, 4 ml of precooled Py monomer and 13.28 g of precooled initiator APS were added to the mixture dropwise. The polymerization reaction was carried out at 0–5 °C for 8 h and kept under room temperature another 12 h. The powder of TiO_2/PPy particles was collected on the filter and rinsed with distilled water several times. In order to decrease the conductivity of PPy coating, the sample was

dispersed in fivefold molar excess of 1 M ammonium hydroxide for 5 h. Then, after filtration, TiO_2/PPy was rinsed with distilled water and dried as above. The weight fraction of PPy in the composite determined by thermogravimetric analysis (Setaram SetSys Evolution 1200, USA) was 34 wt.%.

Particle characterization

The structural analysis of prepared materials was carried out on an X'Pert PRO (Philips, the Netherlands) X-ray diffractometer, fitted with copper target, K_α ray, scanning rate of 4°min^{-1} for the recording data in the range of $2\theta = 20\text{--}80^\circ$ (360 kV, 20 mA). Elicited phase and purity from powder XRD patterns are shown in Fig. 1. All the diffraction peaks can be indexed to a pure tetragonal rutile phase according to JCPDS card No. 21–1276 with lattice constants $a = 4.602 \text{ \AA}$ and $c = 2.956 \text{ \AA}$. In obtained XRD patterns, no other impurity peaks are detected. The peaks are not so sharp, and a small amorphous halo due to PPy appears in TiO_2/PPy particles XRD pattern.

The morphologies of the TiO_2/PPy powder as well as its PPy-coated variants were determined with SEM (Scanning Electron Microscope VEGA II LMU; Tescan, Czech Republic) operated at 10 kV and is shown by scanning electron micrograph in Fig. 2. As can be seen, the particles are hollow globular clusters of TiO_2 primary nanoparticles with the size of around 1 μm . PPy coating can be recognized on the surface.

Preparation of ER fluids

Five, 15, and 25 wt.% of uncoated and PPy-coated hollow globular clusters were dispersed by ultrasonic mixing in silicone oils Lukosiol M15 (Chemical Works Kolín, Czech Republic; viscosity 14.5 mPa s, density 0.965 g cm^{-3}) and Lukosiol M200 (Chemical Works Kolín, Czech Republic;

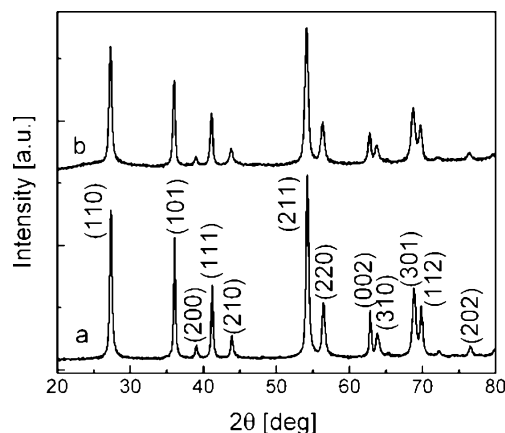
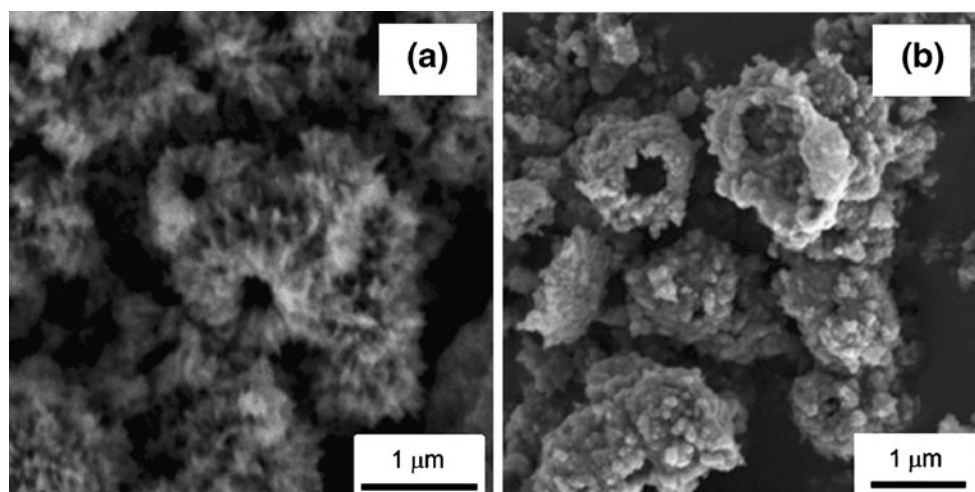


Fig. 1 Powder XRD patterns of the mere TiO_2 clusters (a) and TiO_2/PPy particles (b)

Fig. 2 SEM images of TiO₂ (a) and TiO₂/PPy (b) hollow globular clusters



viscosity 194 mPa s, density 0.965 g cm⁻³). To avoid the influence of moisture, both silicone oils were dried at 80 °C for 24 h.

Electrorheological measurements

The ER properties of the fluids under investigation were measured using a rotational rheometer (Bohlin Gemini, Malvern Instruments, UK), with coaxial cylinder geometry (length 27.4 mm, inner cylinder of 14 mm in diameter and the outer cylinder separated by a 0.7-mm gap), modified for ER experiments. A DC voltage (0.35 until 2.1 kV) corresponded to the electric field strength range 0.5–3 kV mm⁻¹ was generated by a DC high-voltage source TREK (TREK 668B, USA). All steady-flow measurements in the controlled shear rate (CSR) mode were performed in the shear rate range 0.1–300 s⁻¹. The oscillatory tests were carried out through dynamic strain sweeps and frequency sweeps. The strain sweeps were performed in the applied strain range of 10⁻⁴ to 10⁻² at a fixed angular frequency of 6.28 rad s⁻¹ under an electric field in order to get the position of the linear viscoelastic region (LVR). Afterwards, the viscoelastic moduli were obtained from the frequency sweep tests (0.5 to 100 rad s⁻¹) at fixed strain amplitude in the LVR. All the oscillatory measurements were performed in the CSR mode.

In both modes before each measurement at new electric field strength used, the formed internal structure within the suspension was destroyed by shearing of the sample at a shear rate 20 s⁻¹ for 150 s. The temperature in all experiments was kept at 25 °C.

Dielectric properties

Dielectric properties in the frequency range of 40–5 × 10⁶ Hz were measured with an impedance analyzer (Agilent 4524, Japan). Although the Cole–Cole equation has been frequently used for investigation of dielectric

properties of many ER fluids [18], the dielectric spectra (Fig. 3) expressed by complex permittivity ϵ^* were analyzed in this study using Havriliak–Negami equation by which the asymmetry of relaxation peak can be more properly fitted [19]:

$$\epsilon^* = \epsilon'_{\infty} + \frac{(\epsilon'_0 - \epsilon'_{\infty})}{(1 + (i\omega \cdot t_{rel})^a)^b} \quad (1)$$

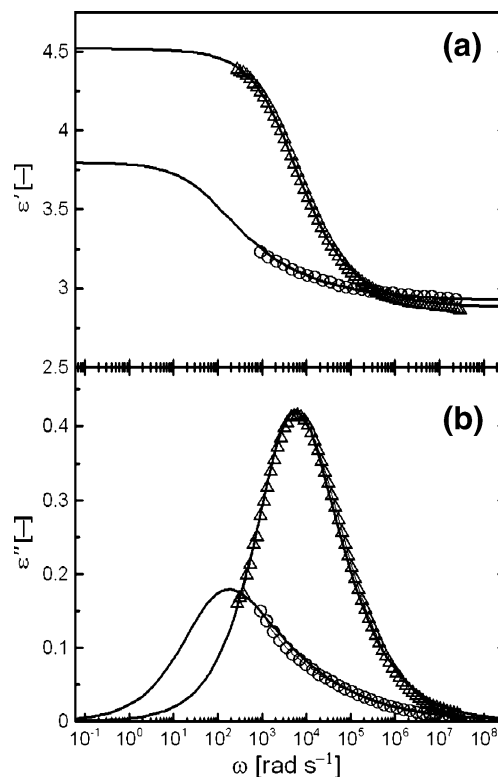


Fig. 3 Relative permittivity, ϵ' , (a) and dielectric loss factor, ϵ'' , (b) as a function of the angular frequency, ω , for 5 wt.% suspension of TiO₂ hollow globular clusters (empty circle) and TiO₂/PPy (empty triangle) particles

where polarizability, $\Delta\epsilon'$, is defined as the difference between static ϵ'_0 and high-frequency ϵ'_∞ relative permittivity, ω is angular frequency, t_{rel} is the relaxation time, and a and b are shape parameters which describe the symmetric and asymmetric broadening of the dielectric function, $0 < a, a \cdot b < 1$. The parameters a and b are related to the limiting behavior of the dielectric function at low and high frequencies. The relaxation frequency, at which the dielectric loss factor ϵ'' has a maximum, is proportional to the rate of polarization of suspension particles.

Sedimentation behavior

Stability of ER fluid consisted of 25 wt.% TiO_2 hollow clusters and their PPy-coated variant in silicone oil M15 was examined by sedimentation ratio test based on a simple naked eye observation of sedimentation velocity (Fig. 4). Within this method, the samples were placed into test tubes and observed for 220 h. The settling of macroscopic phase boundary between the concentrated suspension and the relatively clear oil-rich phase was measured as a function of time. Then, the sedimentation ratio is defined as the height of particle-rich phase relative to the total suspension height. As can be seen, the ER fluids keep stable for a long time because of hollow structure. Furthermore, TiO_2 /PPy suspension exhibits higher sedimentation stability than that of TiO_2 particles based one in the same time period which is caused by improved particles compatibility with the oil medium due to PPy coating.

Results and discussion

ER effect and dielectric properties

Figure 5 illustrates an increase in ER activity of the mere TiO_2 clusters after PPy coating. Almost linear log–log plot

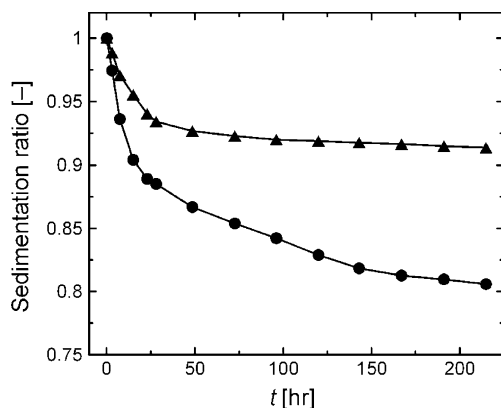


Fig. 4 Sedimentation ratio/time dependence of 25 wt.% ER suspensions of TiO_2 (filled circle) and TiO_2 /PPy (filled triangle) particles in silicone oil M15

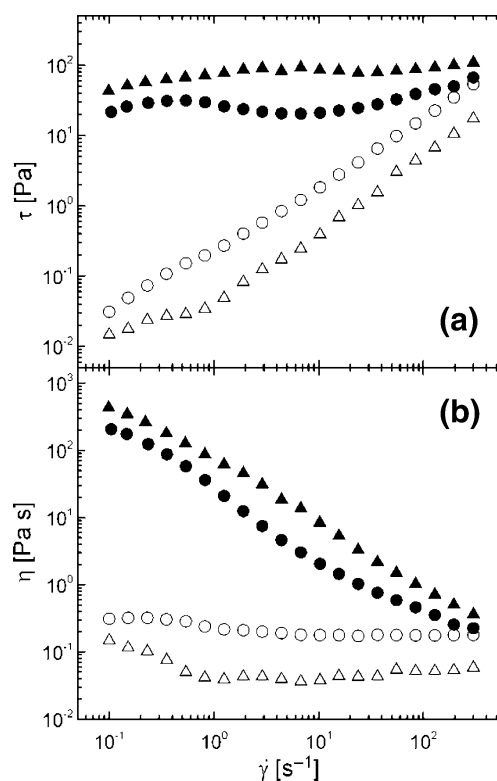


Fig. 5 Double-logarithmic plots of the shear stress, τ , (a) and the viscosity, η , (b) vs. shear rate, $\dot{\gamma}$, for 5 wt.% suspension of TiO_2 (filled circle, empty circle) and TiO_2 /PPy (filled triangle, empty triangle) particles in silicone oil M15. The electric field strengths (in kilovolts per millimeter): 0 (empty circle, empty triangle), 3 (filled circle, filled triangle)

of the shear stress on the rate of shear for suspension of both coated and uncoated particles in the absence of the electric field suggests almost Newtonian behavior characteristic for suspension of non-polarized particles (Fig. 5a). Viscosity of the sample of mere TiO_2 particles predominates (Fig. 5b) probably due to their more hydrophilic surface than PPy layer and, consequently, worse particle compatibility with the hydrophobic oil medium [9, 20]. Under electric field application, the low-shear apparent viscosity of both suspensions increased. The flow became pseudoplastic, and the ER response of PPy-coated particles was higher. As seen in Fig. 5a, the peak in the shear stress develops during shearing of the suspension in the electric field. This phenomenon is attributed to the rearrangement in

Table 1 Parameters in Eq. 1 and polarizability of ER fluids

Parameter	TiO_2	TiO_2 /PPy
ϵ'_0	3.8	4.52
ϵ'_∞	2.92	2.88
$\Delta\epsilon'$	0.88	1.64
t_{rel}	1.63E-02	2.64E-04

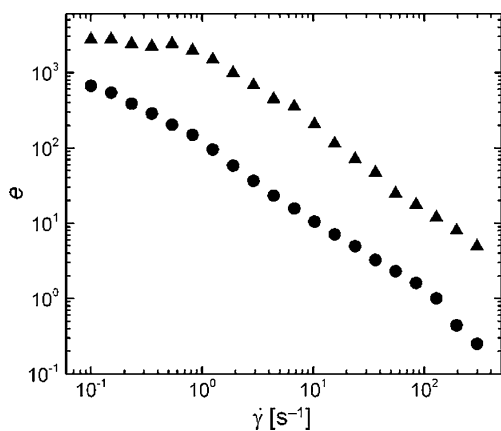


Fig. 6 The dependence of the performance, e , on the shear rate, $\dot{\gamma}$, for 5 wt.% suspension of mere TiO_2 particles (filled circle) and TiO_2/PPy -coated particles (filled triangle) in silicone oil M15

ER structures from chain-like structures spanning the gap between electrodes to lamellar structures as has been demonstrated in several ER fluids [21]. Because the rearrangement requires both electrostatic and hydrodynamic forces, it has been suggested that due to the thermodynamic reasons, the lamellar structures spontaneously form, driven by a lowering of the free energy in the system [22].

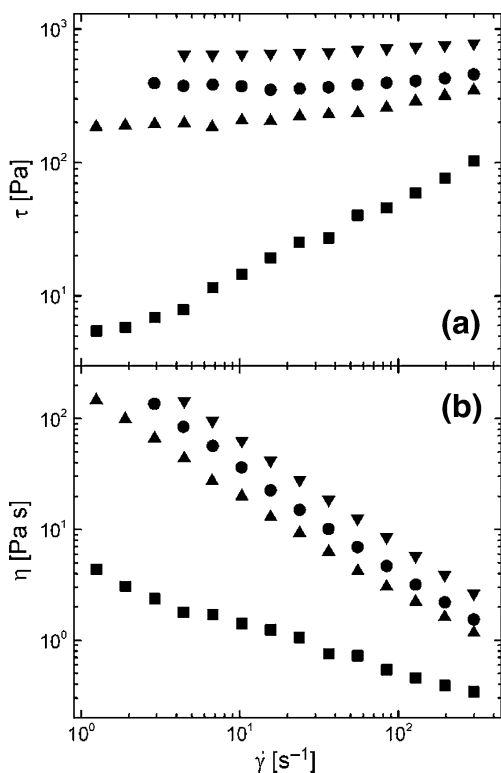


Fig. 7 Double-logarithmic plot of the shear stress, τ , (a) and viscosity, η , (b) vs. shear rate, $\dot{\gamma}$, for 25 wt.% ER fluid of TiO_2/PPy particles in silicone oil M15 at various electric field strengths E (in kilovolts per millimeter): 0 (filled square), 1 (filled triangle), 2 (filled circle), 3 (filled inverted triangle)

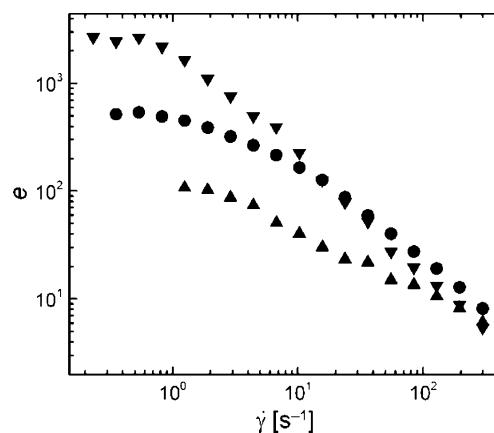


Fig. 8 The dependence of performance, e , on the shear rate, $\dot{\gamma}$, for suspension of TiO_2/PPy particles in silicone oil M15. Particle concentrations (in weight percent): 5 (filled inverted triangle), 15 (filled circle), 25 (filled triangle)

Especially mere TiO_2 hollow globular clusters suspension exhibits during the initial stages of shearing under electric field rearrangement from static aligned particles chain-like structure into another dynamic one.

It is generally accepted that interfacial polarization of particles and formation of chain-like structures in ER materials are closely related to dielectric phenomena. The dielectric spectra (Fig. 3) and their characteristics in the Table 1 indicate that PPy coating of particles enhanced the magnitude of particle polarizability, $\Delta\epsilon'$, and decreased the relaxation time, t_{rel} . As a result, highly polarized particles with higher mobility were organized in a stiffer ER structure of suspension with higher viscosity.

For practical use, in addition to viscosity of suspension reached at the electric field strength used, also electric field-off value must be considered for evaluation of the efficiency of ER phenomenon. Thus, the performance of the ER liquid corresponding to a relative increase in electroviscosity,

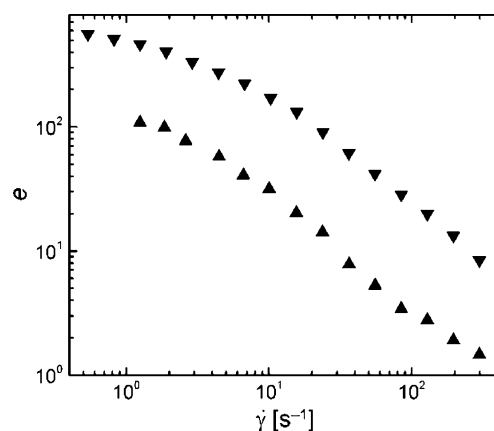


Fig. 9 The dependence of ER performance, e , on the shear rate, $\dot{\gamma}$, of 15 wt.% suspension of TiO_2/PPy particles in M15 (filled inverted triangle) and M200 (filled triangle) silicone oil

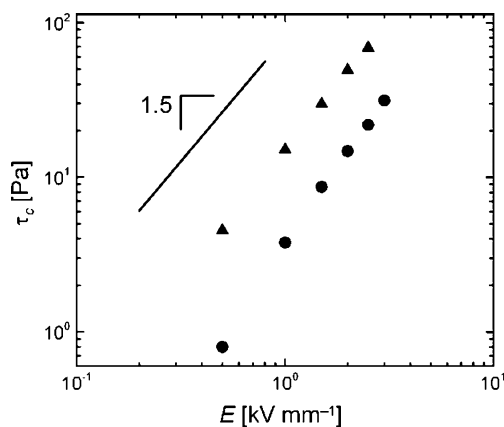


Fig. 10 Double-logarithmic plot of the shear stress, τ_c , vs. electric field strength, E , for 5 wt.% suspension of TiO_2 (filled circle) and TiO_2/PPy (filled triangle) particles in silicone oil M15

$\Delta\eta_E = \eta_E - \eta_0$, due to electric field application can be expressed as $e = (\eta_E - \eta_0)/\eta_0$, where η_E is a viscosity of ER structure [23]. It is worth to noting here the case of nanoparticles-based ER fluids providing a giant ER effect [24]. Unfortunately, no information about ER performance has been found in the literature dealing with such systems. However, one can expect that the ER performance could be comparable with conventionally used ER systems due to very high off-state viscosity of giant ER fluids, which could also be a problem in some practical applications.

In our study it is obvious that the ER efficiency is significantly higher for system based on coated particles due to higher viscosity in the low-shear rate region under electric field applied and lower field-off viscosity (Fig. 6).

Steady-state flow properties

The rigidity of the particles chain structure in suspension of TiO_2/PPy particles under electric field influence steeply increased with particle concentration. The shear stress of

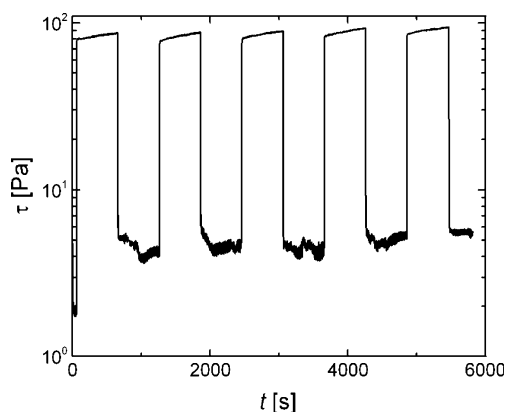


Fig. 11 Time dependence of the shear stress, τ , in the alternate switching on ($E=1.5 \text{ kV mm}^{-1}$)/off regime of 15 wt.% suspension of TiO_2/PPy particles in silicone oil M15 at the constant shear rate $\dot{\gamma} = 5 \text{ s}^{-1}$

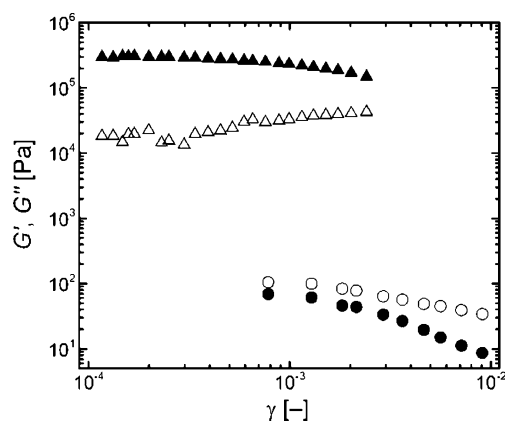


Fig. 12 Storage, G' , (solid symbols) and loss, G'' , (open symbols) moduli vs. strain, γ , at angular frequency 6.28 rad s^{-1} for 25 wt.% suspension of TiO_2/PPy particles in silicone oil M15. Electric field strengths E (in kilovolts per millimeter): 0 (filled circle, empty circle), 3 (filled triangle, empty triangle)

25 wt.% suspension at low shear rates at the field strength 3 kV mm^{-1} reached about 0.7 kPa (Fig. 7). However, due to steeper increase in the field-off value, the performance with particle concentration decreased (Fig. 8).

The higher viscosity of suspension medium caused lower relative increase in electroviscosity and, consequently, lower ER performance (Fig. 9).

The response to the electric field

The determination of the dynamic yield stress by extrapolation of the shear stress to zero shear rate is problematic because of unsteady flow at low shear rates caused by deformation, destruction, and reformation of formed chain-like and columnar ER structures [25]. Thus the shear stresses, τ_c , at the low shear rates $\dot{\gamma}_c = 0.5 \text{ s}^{-1}$ have been

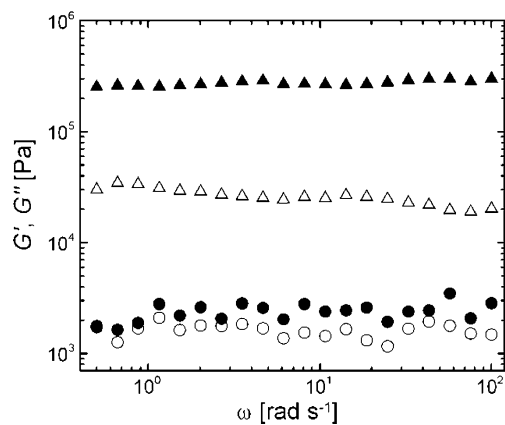


Fig. 13 Storage, G' , (solid symbols) and loss, G'' , (open symbols) moduli vs. angular frequency, ω , for 25 wt.% suspension of TiO_2/PPy particles in silicone oil M15. Electric field strengths E (in kilovolts per millimeter): 0 (filled circle, empty circle), 3 (filled triangle, empty triangle)

used as a criterion of rigidity of static particle chain-like structure. The dependence of this quantity on the electric field strength, E , (Fig. 10) illustrates the improvement in the ER activity of TiO₂ hollow clusters by PPy coating. The linear log–log plot of τ_c vs. E obeys the power law $\tau_c = q E^\alpha$, where the response of particles on the electric field strength $\alpha = 1.46$ – 1.58 corresponds to the theoretical predictions for well-developed ER structure ($\alpha = 1.5$) [26]. The higher q value for suspension of TiO₂/PPy particles confirms strong increase in ER efficiency due to particle coating.

Reproducibility of ER structure

The reproducibility of ER phenomenon is another basic factor for the use of ER liquids in practice. Thus, the alternate switching on and off the electric field should provide the same increase or decrease in suspension viscosity and reach during milliseconds virtually the same ER structure. Figure 11 demonstrates that the shear stress reached after switching on/off cycles with 15 wt.% ER suspension based on TiO₂/PPy particles in silicone oil M15 sheared at 5 s^{-1} and 1.5 kV mm^{-1} fulfills the requirements.

Dynamic oscillatory experiments

The formation of the internal chain-like structure of polarized particles under electric field application is also accompanied by a change of viscoelastic characteristics. Figure 12 depicts the dependence of G' and G'' on the strain amplitude (γ) in oscillatory flow for 25 wt.% TiO₂/PPy particles suspension. Without the electric field, the viscous modulus, G'' , in the suspension is dominant over elastic one, G' . When the electric field is applied, however, G' becomes significantly higher than G'' in the linear viscoelastic region and both moduli increase rapidly in several orders of magnitude from their electric field-off values. When the strain acting on the internal structure increases beyond a certain degree, the elastic and viscous moduli intersect each other ($G' = G''$), the chain structure of the ER fluid breaks rapidly and the system starts to flow [27].

For practical applications it is important to know the moduli in linear viscoelastic region and their angular frequency dependence. Figure 13 presents the change in G' and G'' of 25 wt.% suspension of TiO₂/PPy particles at the small strain of 3×10^{-4} under electric field strength 3 kV mm^{-1} . In the absence of electric field, G' and G'' exhibited the similar values. Relatively high G' is probably due to the presence of irregular shaped TiO₂/PPy particles, which can form aggregates in the flow even in the absence of electric field, and so increase the elastic portion within the ER suspension. Under electric field application, unlike G'' an increase in G' about two orders of magnitude was much

higher. The elastic modulus was substantially larger than the viscous modulus and the ER suspension exhibited solid-like behavior, i.e., G' became nearly independent of frequency. This plateau of the frequency-dependent viscoelastic modulus is a characteristic of aligned 3D microstructures under electric field application [28].

Conclusions

Hollow globular clusters of titanium oxide nanoparticles coated with polypyrrole were prepared as a dispersed phase of a novel ER fluid. The steady-state flow and dynamic measurement showed that unlike mere uncoated particles, their ER efficiency after polypyrrole coating was significantly higher. This result is in good agreement with the dielectric properties indicating higher particles polarizability and lower relaxation frequency. The reproducibility and speed of the formation and breaking of the ER structure met the requirements. The performance characterized by a relative increase in electroviscosity appeared to be significantly affected by particle content and viscosity of suspension medium.

Acknowledgments The authors wish to thank the Ministry of Education, Youth and Sports of the Czech Republic (MSM 7088352101) and the Grant Agency of the Czech Republic (202/09/1626) for financial support. This article was written with support of Operational Programme Research and Development for Innovations cofunded by the European Regional Development Fund (ERDF) and national budget of the Czech Republic, within the framework of Centre of Polymer Systems project (reg. number: CZ.1.05/2.1.00/03.0111).

References

- Papadopoulos CA (1998) Brakes and clutches using ER fluids. *Mechatronics* 8:719–726
- Choi SB, Lee DY (2005) Rotational motion control of a washing machine using electrorheological clutches and brakes. *Proc Inst Mech Eng Part C J Eng Mech Eng Sci* 219:627–637
- Dragasius E, Navickaite S, Rugaityte V (2008) Development and Investigation of Electrorheological Clutch. *Proc 7th Inter Conf Vibroeng* 32–34
- Parthasarathy M, Klingenberg DJ (1996) Electrorheology: mechanisms and models. *Mater Sci Eng R Rep* 17:57–103
- Hao T (2002) Electrorheological fluids. *Adv Colloid Interface Sci* 97:1–35
- Yin JB, Zhao XP (2006) Advances in electrorheological fluids based on inorganic dielectric materials. *J Ind Eng Chem* 12:184–198
- Quadrat O, Stejskal J (2006) Polyaniline in electrorheology. *J Ind Eng Chem* 12:352–361
- Cheng QL, Pavlinek V, He Y, Lengalova A, Li CZ, Saha P (2008) Structural and electrorheological properties of mesoporous silica modified with triethanolamine. *Colloid Surface Physicochem Eng Aspect* 318:169–174
- Stenicka M, Pavlinek V, Saha P, Blinova NV, Stejskal J, Quadrat O (2010) Effect of hydrophilicity of polyaniline particles on their

- electrorheology: steady flow and dynamic behaviour. *J Colloid Interface Sci* 346:236–240
10. Hong CH, Sung JH, Choi HJ (2009) Effects of medium oil on electroresponsive characteristics of chitosan suspensions. *Colloid Polym Sci* 287:583–589
 11. Cheng QL, Pavlinek V, He Y, Yan YF, Li CZ, Saha P (2011) Synthesis and electrorheological characteristics of sea urchin-like TiO₂ hollow spheres. *Colloid Polym Sci* 289:799–805
 12. Yin JB, Zhao XP, Xiang LQ, Xia X, Zhang ZS (2009) Enhanced electrorheology of suspensions containing sea-urchin-like hierarchical Cr-doped titania particles. *Soft Matter* 5:4687–4697
 13. Fang FF, Choi HJ, Ahn WS (2010) Electrorheology of a mesoporous silica having conducting polypyrrole inside expanded pores. *Microporous Mesoporous Mat* 130:338–343
 14. Choi HJ, Jhon MS (2009) Electrorheology of polymers and nanocomposites. *Soft Matter* 5:1562–1567
 15. Liu YD, Fang FF, Choi HJ (2011) Silica nanoparticle decorated polyaniline nanofiber and its electrorheological response. *Soft Matter* 7:2782–2789
 16. Liu FH, Xu GJ, Wu JH, Cheng YC, Guo JJ, Cui P (2010) Synthesis and electrorheological properties of oxalate group-modified amorphous titanium oxide nanoparticles. *Colloid Polym Sci* 288:1739–1744
 17. Li XX, Xiong YJ, Li ZQ, Xie Y (2006) Large-scale fabrication of TiO₂ hierarchical hollow spheres. *Inorg Chem* 45:3493–3495
 18. Liu YD, Fang FF, Choi HJ (2010) Core-shell structured semiconducting PMMA/polyaniline snowman-like anisotropic microparticles and their electrorheology. *Langmuir* 26:12849–12854
 19. Havriliak S, Negami S (1966) A complex plane analysis of alpha-dispersions in some polymer systems. *J Polym Sci C* 16:99–117
 20. Stenicka M, Pavlinek V, Saha P, Blinova NV, Stejskal J, Quadrat O (2011) Structure changes of electrorheological fluids based on polyaniline particles with various hydrophilicities and time dependence of shear stress and conductivity during flow. *Colloid Polym Sci* 289:409–414
 21. Vieira SL, Neto LBP, Arruda ACF (2000) Transient behavior of an electrorheological fluid in shear flow mode. *J Rheol* 44:1139–1149
 22. Henley S, Filisko FE (1999) Flow profiles of electrorheological suspensions: an alternative model for ER activity. *J Rheol* 43:1323–1336
 23. Lengalova A, Pavlinek V, Saha P, Quadrat O, Kitano T, Stejskal J (2003) Influence of particle concentration on the electrorheological efficiency of polyaniline suspensions. *Eur Polym J* 39:641–645
 24. Huang XX, Wen WJ, Yang SH, Sheng P (2006) Mechanisms of the giant electrorheological effect. *Solid State Commun* 139:581–588
 25. Cho MS, Choi HJ, Jhon MS (2005) Shear stress analysis of a semiconducting polymer based electrorheological fluid system. *Polymer* 46:11484–11488
 26. Davis LC (1997) Time-dependent and nonlinear effects in electrorheological fluids. *J Appl Phys* 81:1985–1991
 27. Cheng QL, Pavlinek V, He Y, Li CZ, Saha P (2009) Electrorheological characteristics of polyaniline/titanate composite nanotube suspensions. *Colloid Polym Sci* 287:435–441
 28. Tsuda K, Takeda Y, Ogura H, Otsubo Y (2007) Electrorheological behavior of whisker suspensions under oscillatory shear. *Colloid Surface Physicochem Eng Aspect* 299:262–267